ACR No. E5C30

25 MAR 1948

NATIONAL ADVISORY COMMITTEE FOR AERONAUTICS

WARTIME REPORT

ORIGINALLY ISSUED

April 1945 as
Advance Confidential Report E5C30

EFFICIENCY TESTS OF A SINGLE-STAGE IMPULSE TURBINE HAVING AN 11.0-INCH PITCH-LINE DIAMETER WHEEL WITH AIR AS THE DRIVING FLUID

By David S. Gabriel and L. Robert Carman

Aircraft Engine Research Laboratory
Cleveland, Ohio

WASHINGTON

NACA WARTIME REPORTS are reprints of papers originally issued to provide rapid distribution of advance research results to an authorized group requiring them for the war effort. They were previously held under a security status but are now unclassified. Some of these reports were not technically edited. All have been reproduced without change in order to expedite general distribution.

NACA LIBRARY
LANGLEY MEMORIAL AERONAUTICAL
LABORATORY
Langley Field, Va.

E-216

3 1176 01354 1801

NACA ACR No. E5C30

NATIONAL ADVISORY COMMITTEE FOR AERONAUTICS

ADVANCE CONFIDENTIAL REPORT

EFFICIENCY TESTS OF A SINGLE-STAGE IMPULSE TURBINE HAVING AN 11.0-INCH PITCH-LINE DIAMETER WHEEL WITH AIR AS THE DRIVING FLUID

By David S. Gabriel and L. Robert Carman

SUMMARY

Results are presented of efficiency tests on a single-stage impulse turbine having an 11.0-inch pitch-line diameter wheel and a fabricated nozzle diaphragm using air at moderate temperatures as the driving fluid. Efficiency curves are shown for turbine pressure ratios from 1.2 to 5.2. The maximum efficiency occurred at a blade-to-jet speed ratio of approximately 0.4 and was about 0.615 for turbine pressure ratios from 3.0 to 4.6. Additional curves of the air-flow data are presented.

INTRODUCTION

Research is planned by the Cleveland laboratory of the NACA to determine the efficiency of turbines, turbosuperchargers, and jet-propulsion units. One of the first requirements of the turbine-research program is to develop a tentative standard method of testing these turbines and an accurate and convenient means of presenting the data. Before a tentative standard method can be recommended, it is necessary to collect data under a wide variety of operating conditions and with various types of test installation.

Superheated steam, high-temperature combustion products of an exhaust-gas producer, and engine-exhaust gases have been used as the driving fluid in tests of exhaust-gas turbines. The use of steam and combustion products, however, results in high operating temperatures with accompanying thermal stresses and expansions in equipment. As a result, the gas ducting must be designed for these

factors and corrosion-resistant materials must be specified. The use of hot gas requires special equipment for obtaining the temperature of the driving fluid and increases the difficulty of handling it, particularly when flow surveys and observations are desired.

When air instead of hot gases is used as the driving fluid, a wider range of turbine blade-to-jet speed ratios may be investigated at high turbine pressure ratios without exceeding the maximum wheel speed. The use of cool air as a driving medium, however, may result in different values of turbine efficiency than the values obtained with hot exhaust gas because of the difference in the physical properties of the gases, in the effect of temperature on the structure, and in the heat losses. In addition, complications may be introduced by the condensation of water vapor and formation of ice during the expansion.

An investigation of turbine efficiencies was conducted at the NACA laboratory in Cleveland, Ohio, using air at room temperature as the driving fluid as part of a program to determine whether the turbine performance characteristics obtained in such tests accurately reproduce the results of tests using products of combustion at engine-exhaust temperatures.

APPARATUS AND METHOD

The equipment tested was a single-stage impulse turbine having an 11.0-inch pitch-line diameter wheel with inserted buckets and a fabricated nozzle diaphragm. Bucket-to-nozzle clearance was set at 0.11 to 0.12 inch. The turbine was driven by atmospheric air drawn through it by the laboratory altitude-exhaust system. A high-speed hydraulic dynamometer was coupled to the turbine shaft to absorb the power delivered. The arrangement of the apparatus is shown in figures 1 and 2.

Leakage of air from the atmosphere through the turbine into the low-pressure exhaust was prevented by a housing around the turbine-bearing assembly and plugs welded into the annular spaces between the nozzle box and the nozzle-box baffle. Leakage of air into the housing was prevented by equalizing the pressure across a labyrinth seal gland installed around the turbine shaft between the housing and a chamber evacuated by a controllable jet pump.

The turbine discharged into a plenum chamber, the static pressure of which was taken as the bucket discharge pressure p_d. The bucket discharge pressure was varied by regulating the altitude

exhaust pressure. The static-pressure tap for measuring the discharge pressure was located about 1/2 inch behind the external cooling cap, as shown in figure 2(a). The end of the pressure-tap tube was plugged and a hole was drilled about 1/4 inch from the end of the tube on the downstream side. The cooling caps were installed to reproduce the conditions for turbine tests with hot gases but were not needed for cooling in the air tests.

Dynamometer torque measurements were made with a calibrated beam scale. The turbine speed was measured with a balanced-bridge condenser-type tachometer driven from the standard turbine take-off. The details of the turbine inlet pipe are shown in figure 2(b). An orifice plate was used to measure the air flow. The air temperature, assumed to be the total temperature at the nozzle-box inlet, was measured with a quadruple-shielded chromel-alumel thermocouple and a self-balancing potentiometer. The static pressure at the nozzle-box inlet was measured from a manifold connected to four pressure taps in the same cross section of the inlet pipe.

Turbine-shaft torque was measured to the nearest 0.1 foot-pound. The turbine-speed measurements were accurate to ±20 rpm. The probable error of the air-flow measurements was ±1 percent. The nozzle-box-temperature measurements were accurate to within 3° F. All pressures were measured with mercury manometers to the nearest millimeter of mercury. The locations of the various pressure taps are shown in figure 2.

Efficiency tests were made over the following range of conditions: The ratio of the nozzle-box inlet pressure to the discharge pressure was varied from approximately 1.2 to approximately 5.2; at each pressure ratio, the turbine speed was varied from approximately 2000 to approximately 21,000 rpm to give blade-to-jet speed ratios of 0.1 to 0.7.

The following measurements were taken:

(a) Turbine torque
(b) Turbine speed
(c) Mass flow of air
(d) Nozzle-box total temperature
(e) Nozzle-box inlet static pressure
(f) Static pressure in the plenum chamber

SYMBOLS

A discharge area of the theoretical convergent nozzle, (sq ft)

A_e effective nozzle area, (sq ft)

g acceleration due to gravity, 32.2 (ft)/(sec)^2 or dimensional constant, 32.2 (lb)/(slug)

M_a mass flow of air, (slugs)/(sec)

N turbine speed, (rpm)

p_d static pressure of turbine discharge at plenum chamber, (in. Hg absolute)

p_i total pressure at nozzle-box inlet, (in. Hg absolute)

P_t turbine shaft power, (ft-lb)/(sec)

R_a gas constant, 53.35 (ft-lb)/(lb)($^{\circ}$F)

T_i total temperature at nozzle-box inlet, ($^{\circ}$F absolute)

u blade pitch-line velocity, (fps)

v theoretical jet speed, (fps)

W_{th} available energy, (ft-lb)/(lb)

γ ratio of specific heat at constant pressure to specific heat at constant volume, 1.40

η turbine efficiency

ρ_i density based on nozzle-box inlet total pressure and temperature, (slug)/(cu ft)

ρ_d discharge density at the theoretical convergent nozzle, (slug)/(cu ft)

METHOD OF CALCULATION

The energy available for turbine work was calculated from the total pressure p_i and temperature T_i at the nozzle-box inlet

and the static pressure in the discharge pipe p_d. Velocity head at the nozzle-box inlet was calculated from the inlet static pressure, the inlet total temperature, the mass-flow measurements, and the compressible-flow equations. The velocity head was added to the measured static pressure to give the nozzle-box inlet total pressure. The turbine pressure ratio was then defined as the ratio p_i/p_d. The available energy is given by the expression

$$W_{th} = \frac{\gamma}{\gamma-1} R_a T_i \left[1 - (p_d/p_i)^{\frac{\gamma-1}{\gamma}}\right] \tag{1}$$

The turbine efficiency η is the ratio of the measured turbine power output to the calculated rate of available energy input:

$$\eta = P_t/(gM_a W_{th}) \tag{2}$$

In the computation of turbine blade-to-jet speed ratio, the theoretical jet speed v is the velocity equivalent of the available energy. The blade speed was taken as the turbine pitch-line velocity u. The blade-to-jet speed ratio may be expressed as

$$\frac{u}{v} = \frac{u}{\sqrt{2\, g\, \frac{\gamma}{\gamma-1} R_a T_i \left[1 - (p_d/p_i)^{\frac{\gamma-1}{\gamma}}\right]}} \tag{3}$$

Curves of the air flow through the turbine are also necessary for the computation of the turbine power. The principle variables involved in the mass flow are revealed by a consideration of the continuity equation of the isentropic flow through a convergent nozzle

$$M_a = 70.75\, \frac{p_i}{gR_a T_i}\left(\frac{p_d}{p_i}\right)^{\frac{1}{\gamma}} A \sqrt{2g\, \frac{\gamma}{\gamma-1} R_a T_i \left[1 - \left(\frac{p_d}{p_i}\right)^{\frac{\gamma-1}{\gamma}}\right]} \tag{4}$$

or

$$\frac{M_a}{p_i} \sqrt{gR_a T_i} = f(p_i/p_d)$$

An additional variable is introduced by the interference of the turbine wheel with the flow. A reasonable assumption is that this interference is a function of the blade-to-jet speed ratio. Consideration of equation (3) shows that the only new variable introduced by the blade-to-jet speed ratio is the turbine speed N. The blade-to-jet speed ratio for a given pressure ratio is proportional to the factor $N\sqrt{519/T_i}$. The mass-flow data will be presented by a plot of the factor $\frac{M_a}{p_i}\sqrt{gR_aT_i}$ against p_i/p_d and $N\sqrt{519/T_i}$.

An effective area can be defined as the area of a convergent nozzle, which gives the measured mass flow for the measured values of p_i, T_i, and p_d. Above the critical pressure ratio the mass flow through a convergent nozzle is independent of the pressure ratio. The effective nozzle area can be defined for pressure ratios above critical by the following relation:

$$\frac{M_a}{p_i}\sqrt{gR_aT_i} = \left(\frac{2}{\gamma+1}\right)^{\frac{1}{\gamma-1}} A_e\sqrt{2\,\frac{\gamma}{\gamma+1}} \tag{5}$$

RESULTS AND DISCUSSION

Figure 3 shows the variation of turbine efficiency with blade-to-jet speed ratio over a range of turbine pressure ratios p_i/p_d from 1.23 to 5.22. The curves of figure 3 are parabolic. The maximum efficiency occurred at blade-to-jet speed ratios of approximately 0.4 for all turbine pressure ratios. Slight variations from the required turbine pressure ratio at each blade-to-jet speed ratio were corrected by cross-plotting the data against turbine pressure ratio for constant blade-to-jet speed ratio. The correction was found to be negligible in most cases and was used for only the highest turbine pressure ratio of 5.22.

The maximum efficiency is cross-plotted against turbine pressure ratio in figure 4. The curve rises gradually between pressure ratios from 1.0 to 3.0, is flat from 3.0 to 4.6, and falls off slightly beyond 4.6. The maximum efficiency of 0.615 is reached between pressure ratios of 3.0 and 4.6. The familiar pin-wheel diagram of turbine pressure ratio plotted against blade-to-jet speed ratio for various efficiencies is shown in figure 5.

A plot of the air-flow factor $\frac{M_a}{p_1}\sqrt{gR_aT_1}$ against the ratio $N\sqrt{519/T_1}$ for various turbine pressure ratios p_1/p_d is shown in figure 6. The wheel-speed effect is apparent at low pressure ratios but disappears at pressure ratios above 2.3. A cross plot of figure 6 is shown in figure 7. The air-flow factor is plotted against the pressure ratio for various values of $N\sqrt{519/T_1}$. The air-flow factor becomes constant at a value of 3.04 for pressure ratios between 2.3 and 5.2.

The effective area A_e calculated from equation (5) and the data shown in figure 6 gives a value of 9.02 square inches for pressure ratios greater than 2.3. This area is 82.8 percent of the measured nozzle discharge area.

Unpublished results of NACA tests using compressed air as the driving fluid have shown that icing of the buckets may occur at turbine pressure ratios of 1.6. No unusual operating characteristics indicating progressive icing of the turbine buckets were observed during the tests reported herein. Subsequent unpublished NACA test results have shown that nozzle-box inlet pipes may influence the turbine efficiency to a considerable degree.

SUMMARY OF RESULTS

Tests of a single-stage impulse turbine having an 11.0-inch pitch-line diameter wheel with inserted buckets and a fabricated nozzle diaphragm using air at moderate temperatures as the driving fluid showed that:

1. Maximum efficiency occurred at a blade-to-jet speed ratio of approximately 0.4 for pressure ratios from 1.2 to 5.2.

2. Maximum efficiency was approximately 0.615 for turbine pressure ratios from 3.0 to 4.6.

3. The ratio of the effective area of the turbine (considered as a convergent nozzle) to the true area is 0.828 for pressure ratios above 2.3.

Aircraft Engine Research Laboratory,
National Advisory Committee for Aeronautics,
Cleveland, Ohio.

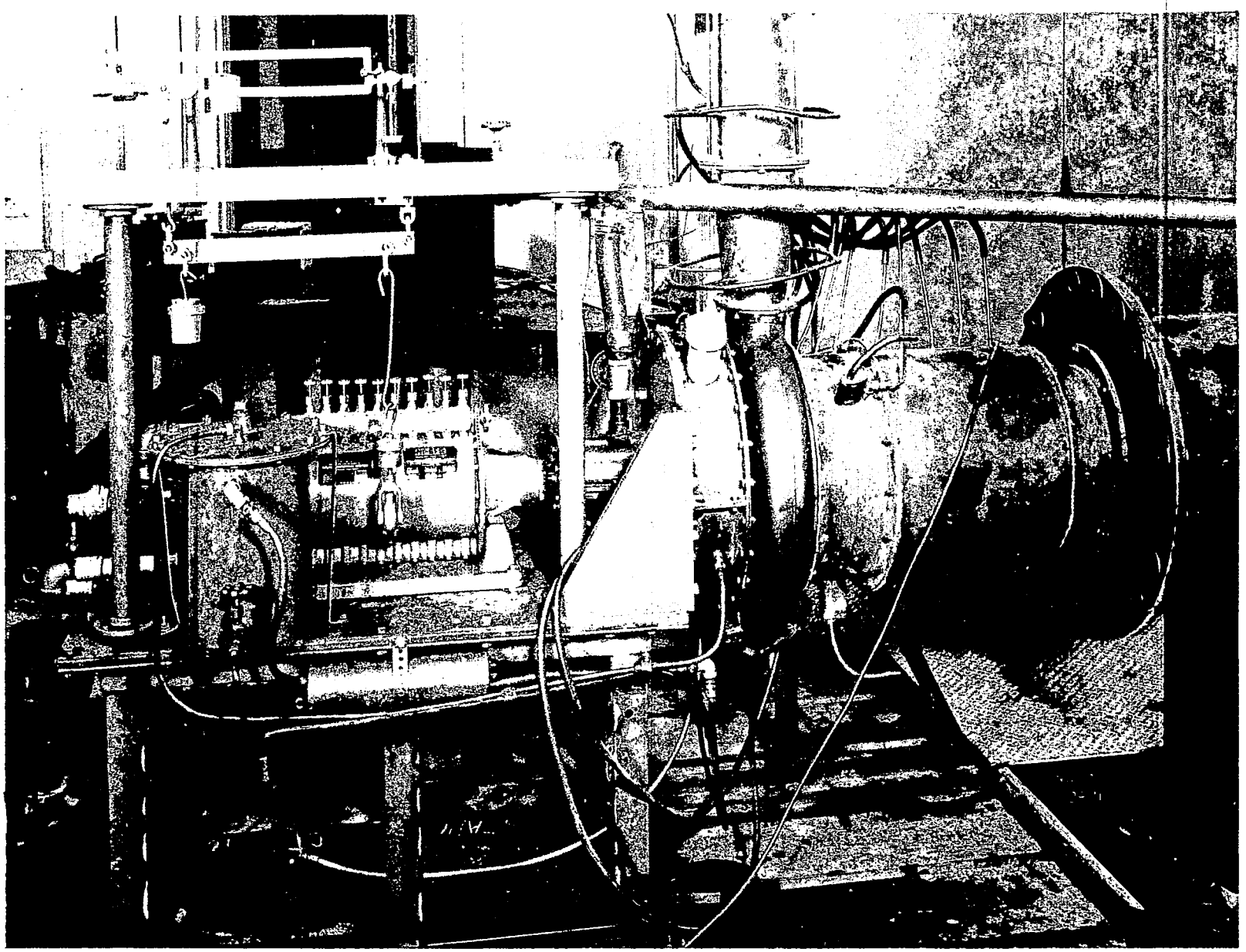

Figure 1. - Turbine testing setup.

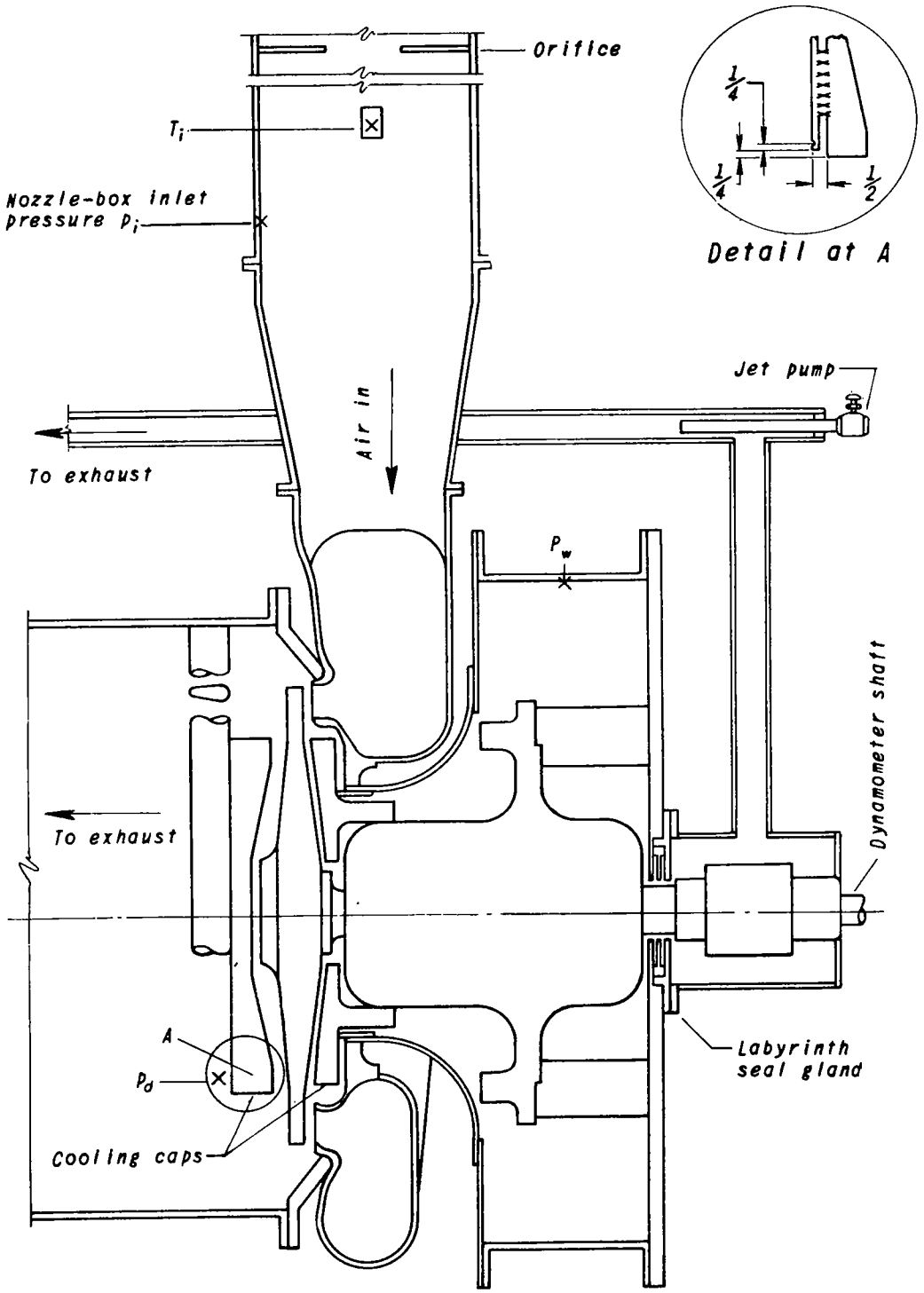

(a) General test setup.

NATIONAL ADVISORY COMMITTEE FOR AERONAUTICS

Figure 2. - Schematic diagram of test apparatus.

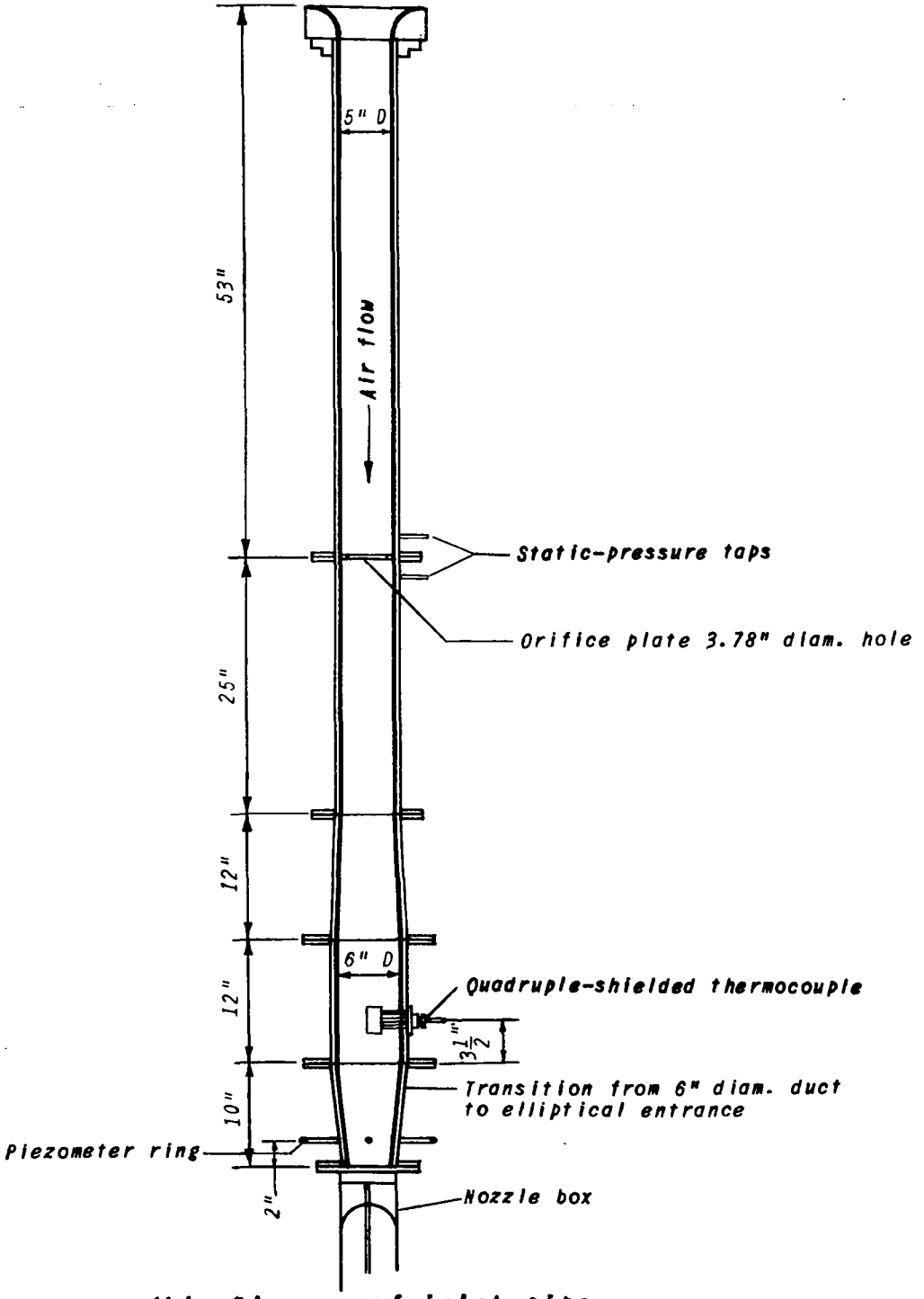

(b) Diagram of inlet pipe.

Figure 2. - Concluded. Schematic diagram of test apparatus.

NATIONAL ADVISORY
COMMITTEE FOR AERONAUTICS

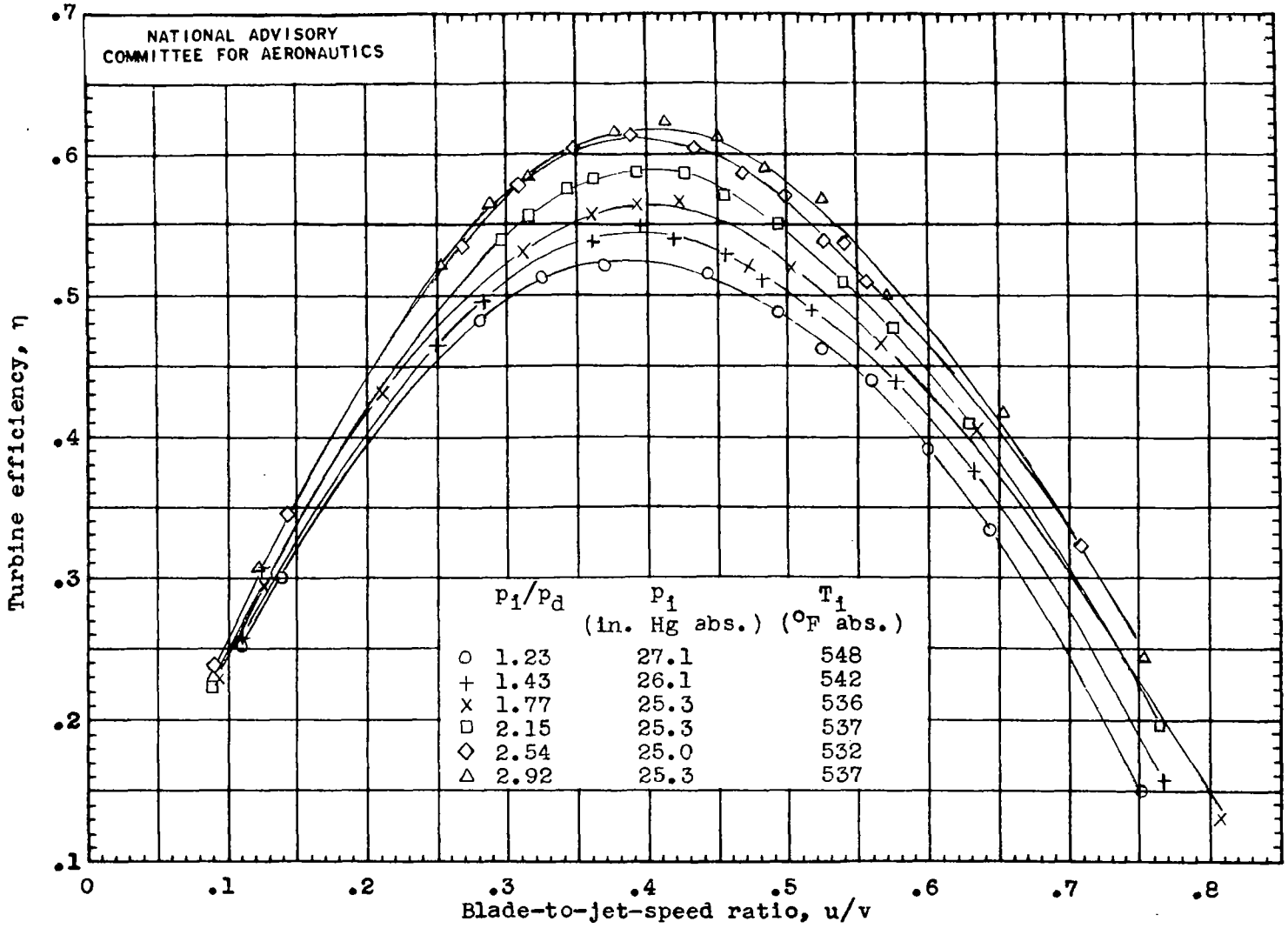

Figure 3.- Variation of turbine efficiency with blade-to-jet-speed ratio for various turbine pressure ratios.

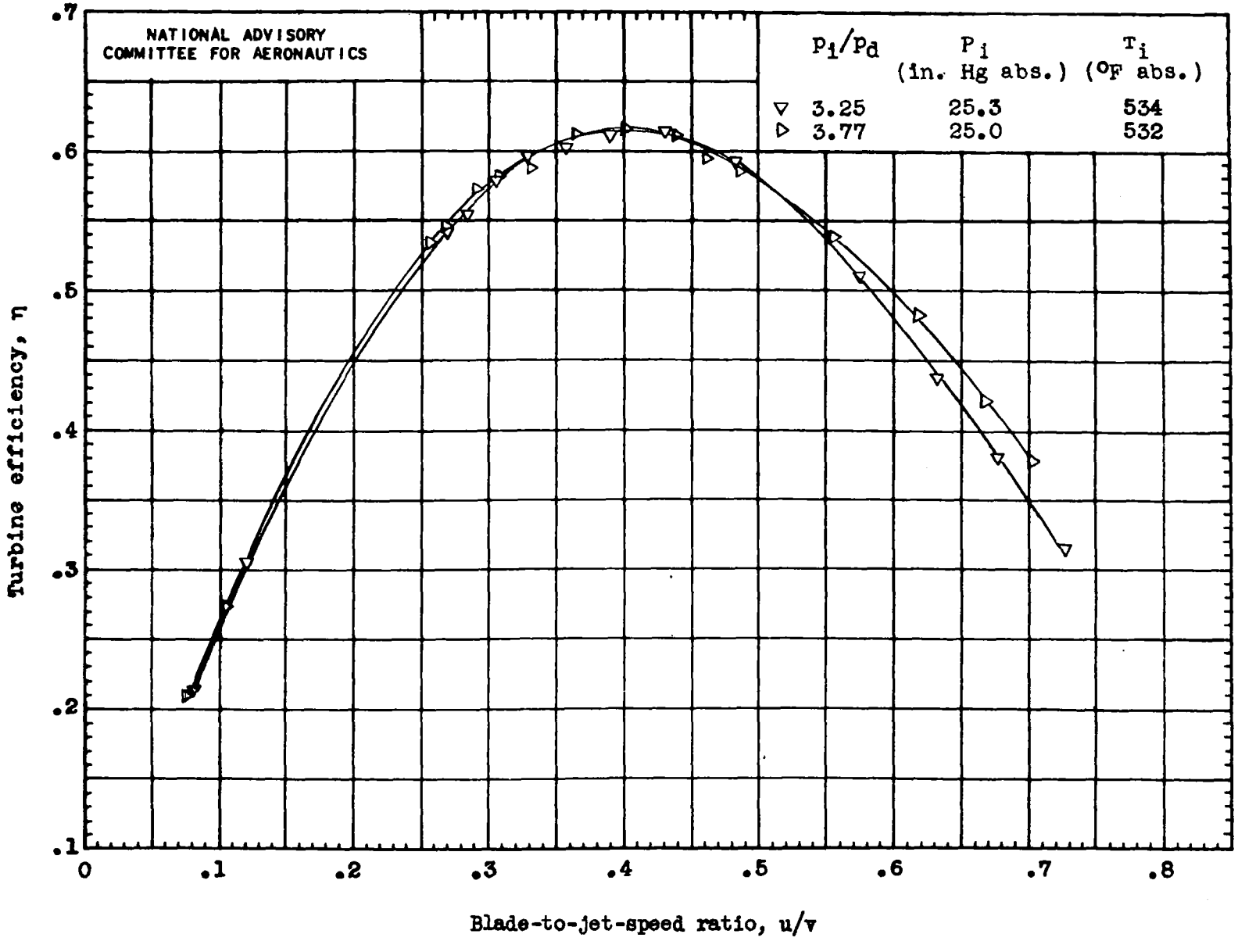

Figure 3. - Continued. Variation of turbine efficiency with blade-to-jet-speed ratio for various turbine pressure ratios.

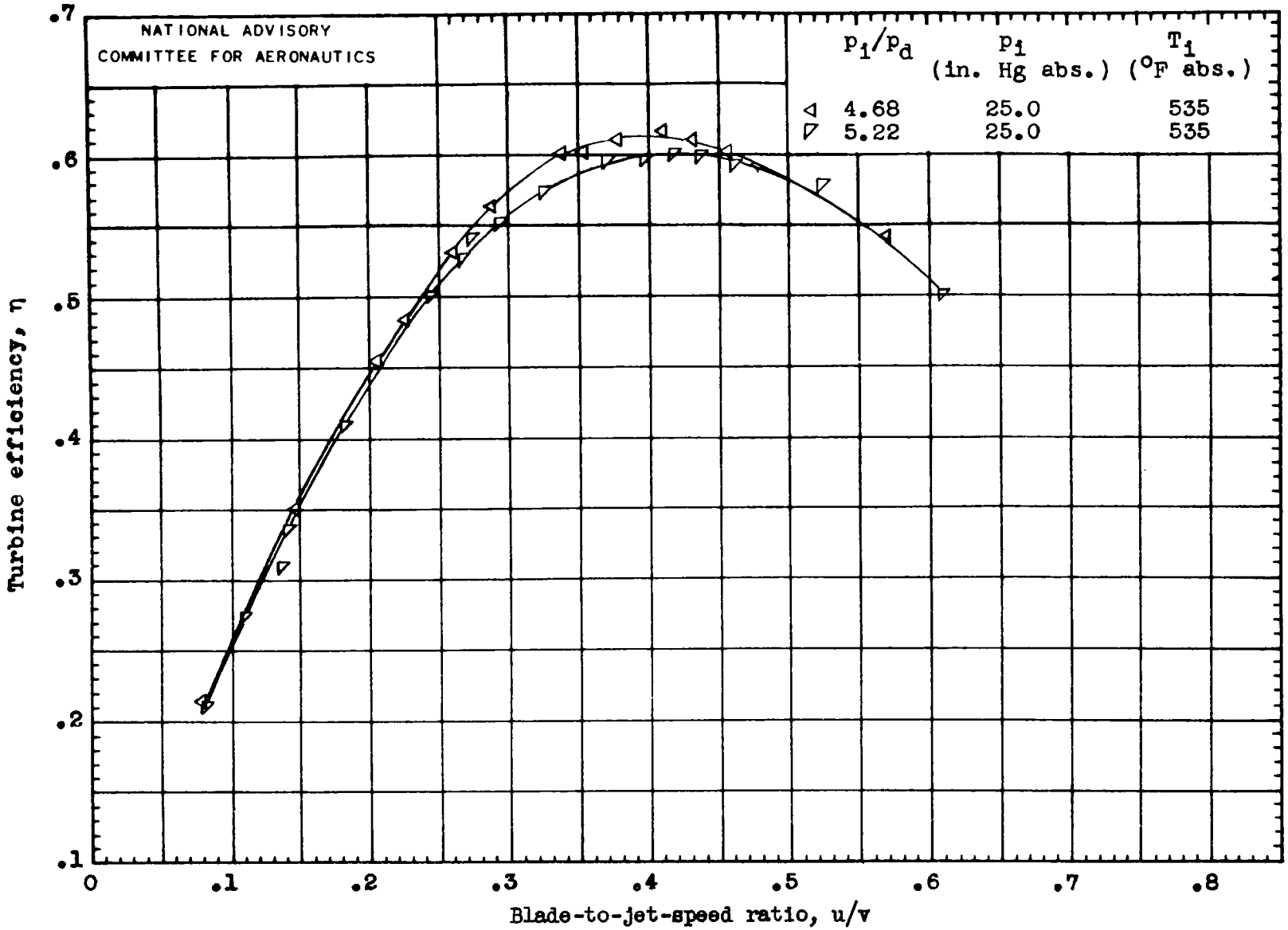

Figure 3. - Concluded. Variation of turbine efficiency with blade-to-jet-speed ratio for various turbine pressure ratios.

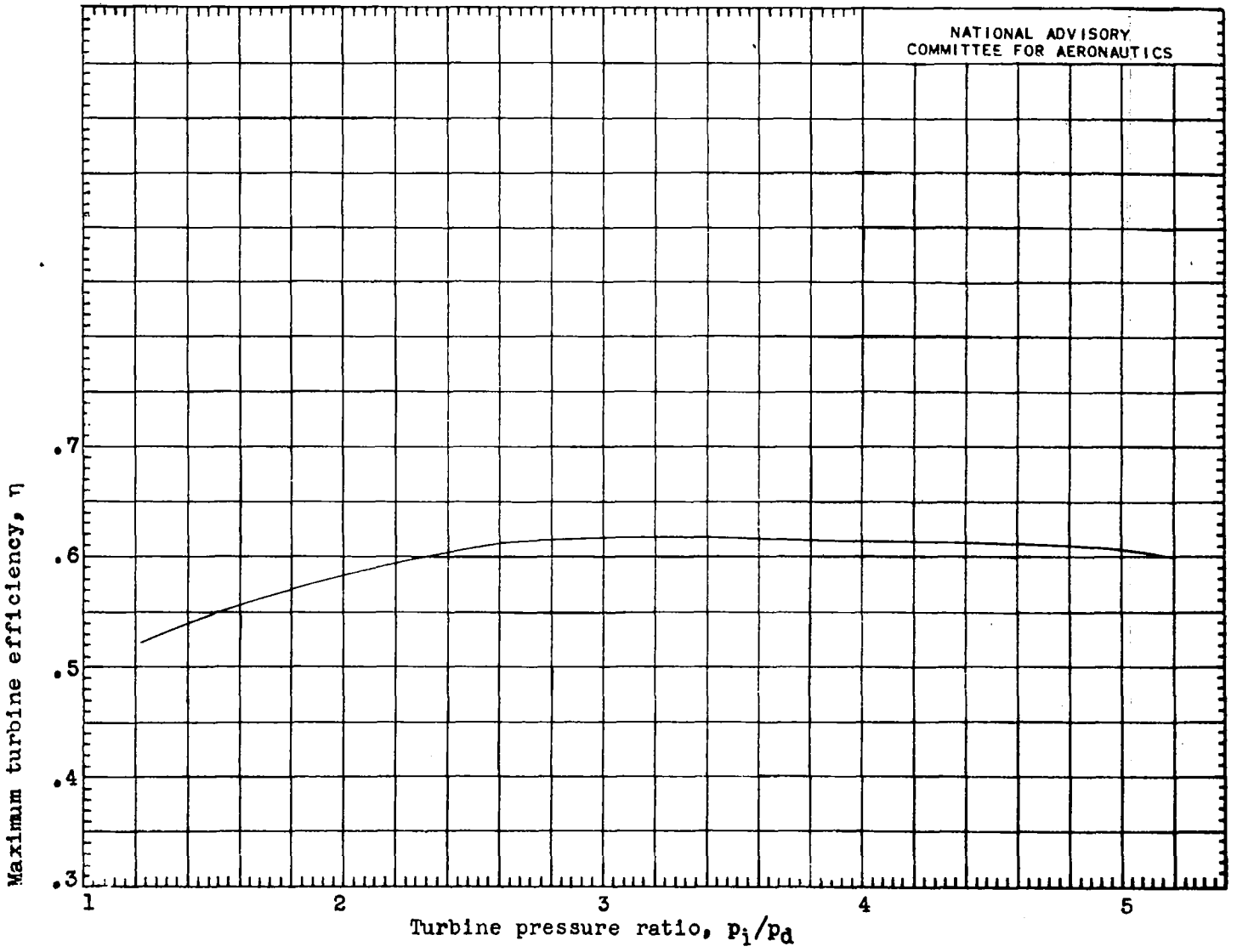

Figure 4.- Variation of maximum turbine efficiency with pressure ratio.

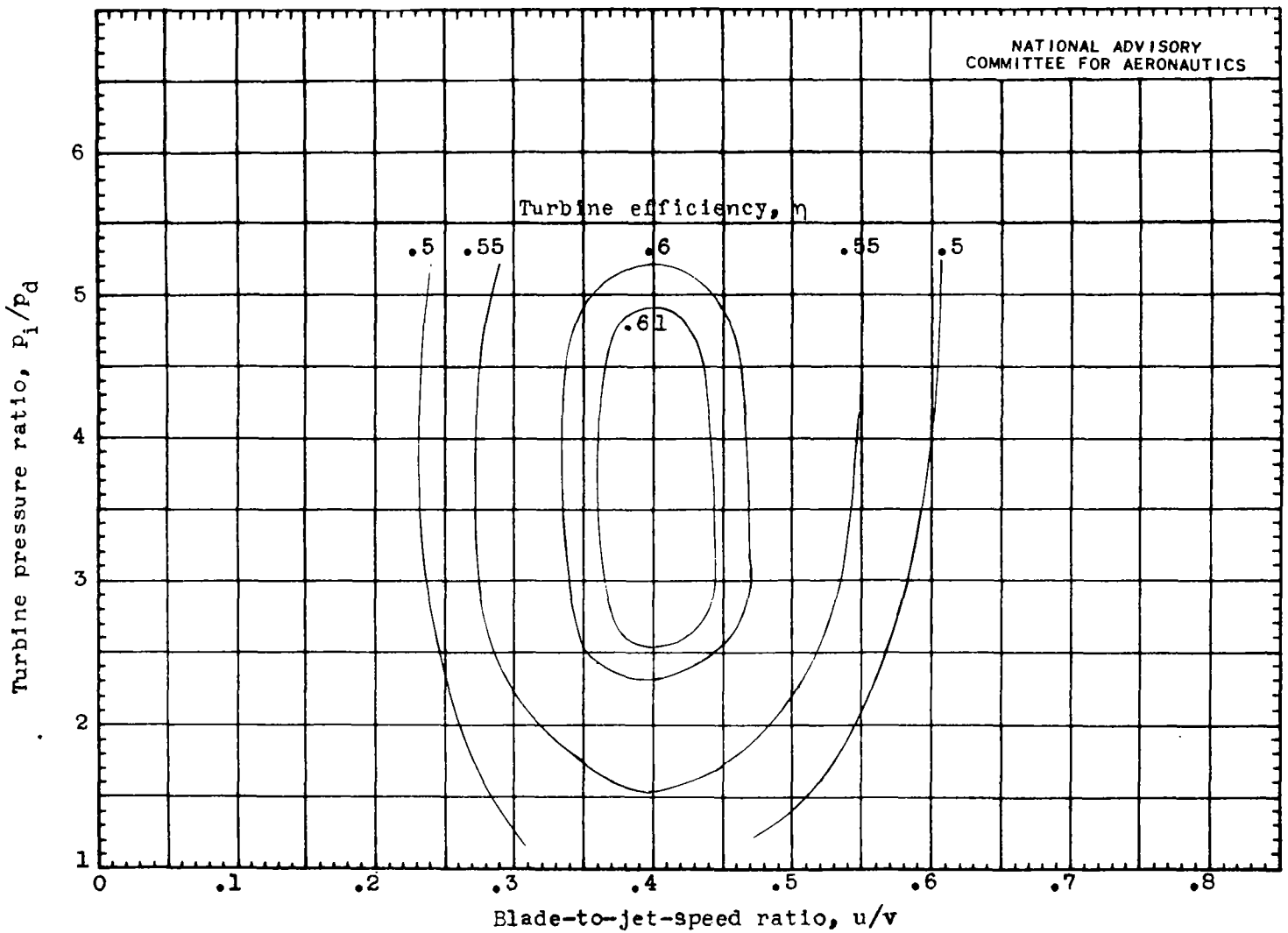

Figure 5.- Relation of pressure ratio to blade-to-jet-speed ratio for various turbine efficiencies.

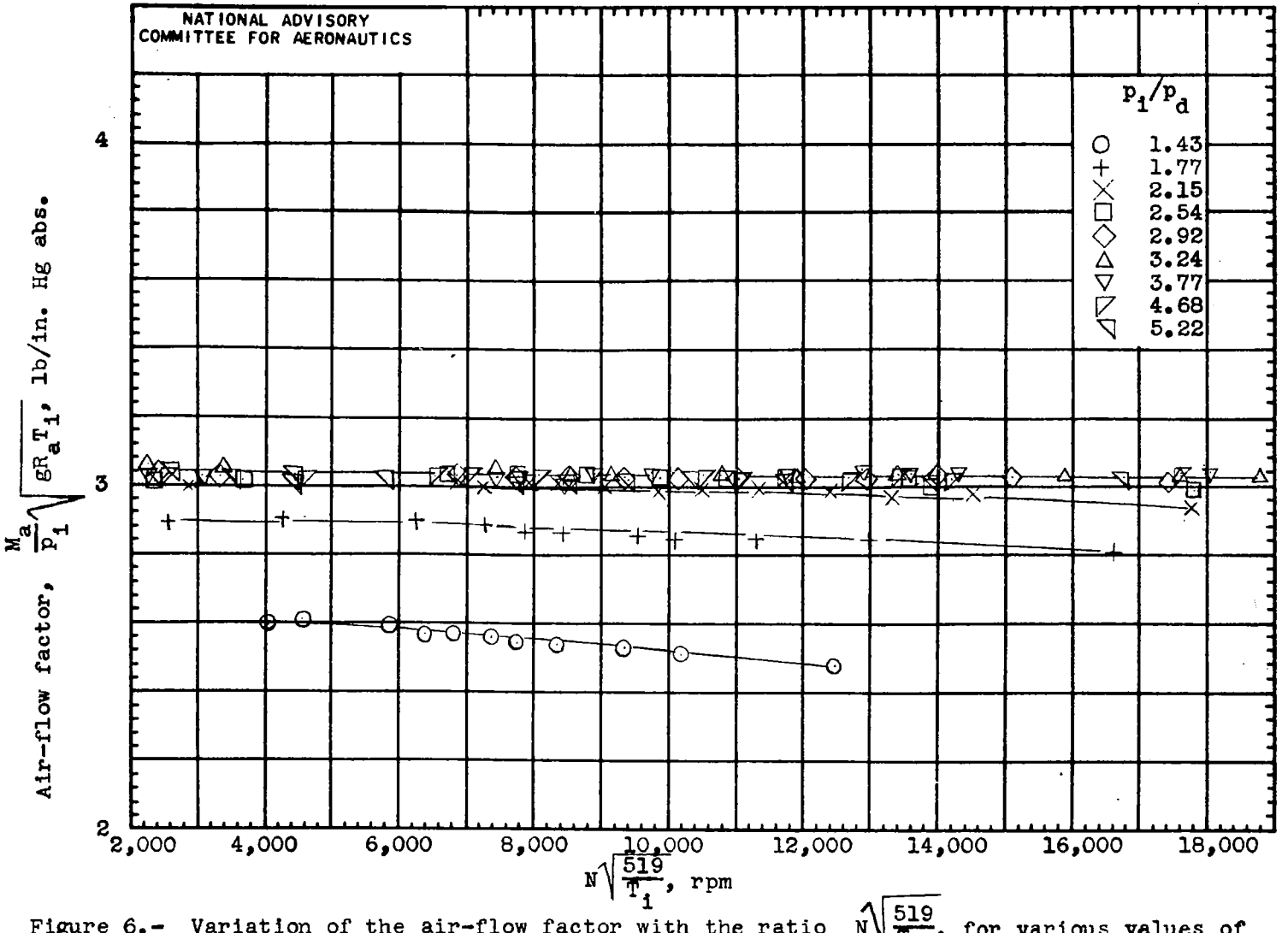

Figure 6.- Variation of the air-flow factor with the ratio $N\sqrt{\frac{519}{T_1}}$, for various values of the pressure ratio p_1/p_d.

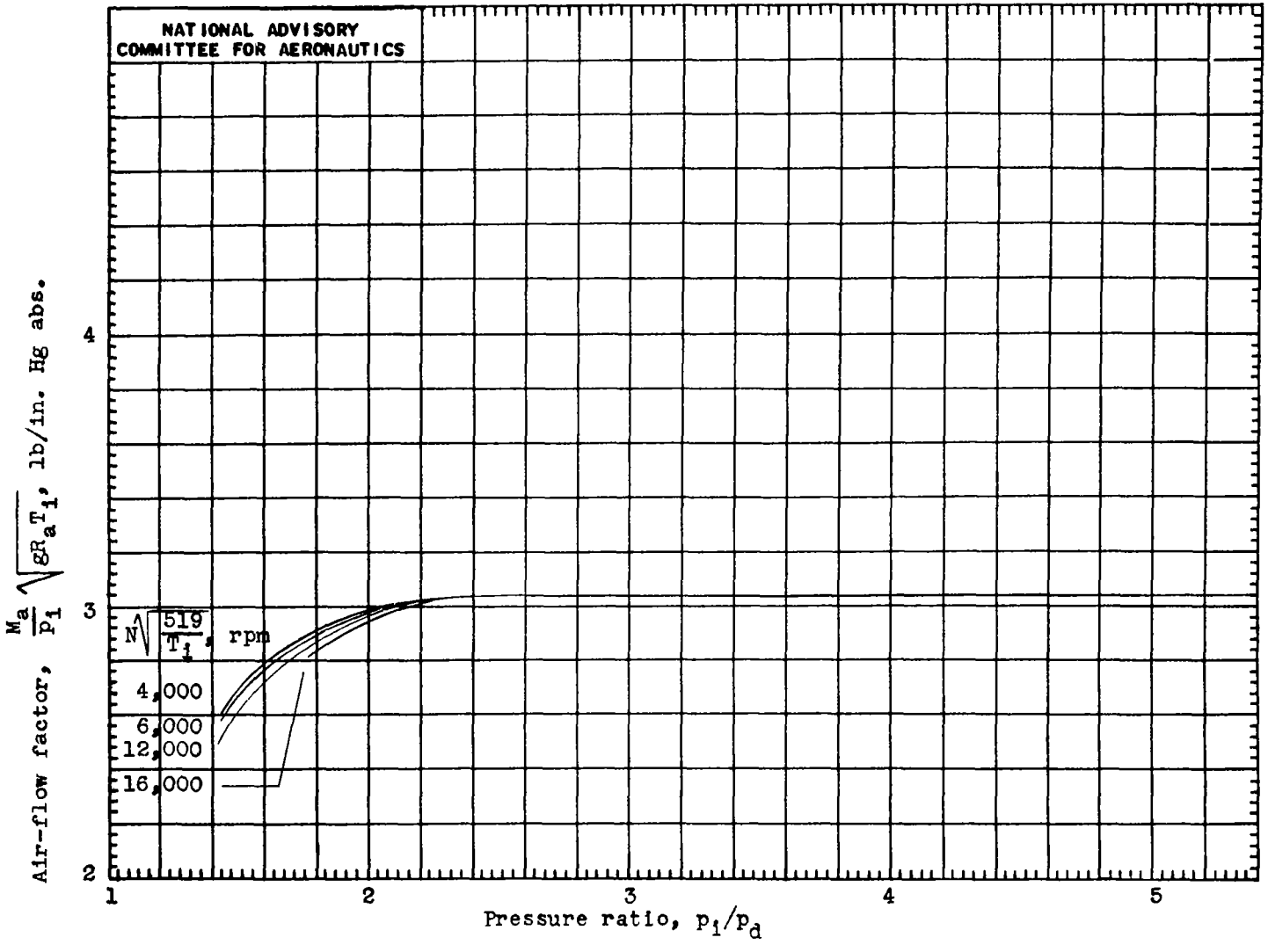

Figure 7.- Variation of the air-flow factor with the pressure ratio for various values of the ratio $N\sqrt{\frac{519}{T_1}}$.

LANGLEY RESEARCH CENTER
3 1176 01354 1801